

Exclusive Baryonic B Decays Circa 2005

Hai-Yang Cheng

Institute of Physics, Academia Sinica
Taipei, Taiwan 115, Republic of China

Abstract

The status of exclusive two-body and three-body baryonic B decays is reviewed. The threshold enhancement effect in the dibaryon invariant mass and the angular distributions in the dibaryon rest frame are stressed and explained. Weak radiative baryonic B decays mediated by the electromagnetic penguin process $b \rightarrow s\gamma$ are discussed. Puzzles with the correlation observed in $B^- \rightarrow p\bar{p}K^-$ decay and the unexpectedly large rate observed for $B \rightarrow \Lambda_c \bar{\Lambda}_c K$ are examined. The former may indicate that the $p\bar{p}$ system is produced through some intermediate states, while the latter implies the failure of naive factorization for $\Lambda\bar{\Lambda}K$ modes and may hint at the importance of final-state rescattering effects.

I. INTRODUCTION

A unique feature of hadronic B decays is that the B meson is heavy enough to allow a baryon-antibaryon pair production in the final state.¹ During the Lepton-Photon Conference in 1987, ARGUS announced the first measurement of the decay modes $p\bar{p}\pi^\pm$ and $p\bar{p}\pi^+\pi^-$ in B decays at the level of 10^{-4} [2]. Although this evidence of charmless baryonic B decays was immediately ruled out by CLEO [3], it nevertheless has stimulated extensive theoretical studies during the period of 1988-1992. Several different model frameworks have been proposed: the constituent quark model [4], the pole model [5, 6], the QCD sum rule [7], the diquark model [8] and flavor symmetry considerations [9].

However, experimental and theoretical activities towards baryonic B decays suddenly faded away after 1992. This situation was dramatically changed in the past five years. Interest in this area was revitalized by many new measurements at CLEO, Belle and BaBar followed by active theoretical studies.

In this talk we would like to give an overview of the experimental and theoretical status of exclusive baryonic B decays by the end of 2005.

TABLE I: Experimental upper limits on the branching ratios of charmless two-body baryonic B decays.

| Decay | BaBar [10, 11] | Belle [12] | CLEO [13] |
|--|----------------------|----------------------|----------------------|
| $\bar{B}^0 \rightarrow p\bar{p}$ | 2.7×10^{-7} | 4.1×10^{-7} | 1.4×10^{-6} |
| $\bar{B}^0 \rightarrow \Lambda\bar{\Lambda}$ | | 6.9×10^{-7} | 1.2×10^{-6} |
| $B^- \rightarrow \Lambda\bar{p}$ | | 4.9×10^{-7} | 1.5×10^{-6} |
| $B^- \rightarrow \Lambda(1520)\bar{p}$ | 1.5×10^{-6} | | |
| $B^- \rightarrow p\bar{\Delta}^{--}$ | | | 1.5×10^{-4} |
| $B^- \rightarrow \Delta^0\bar{p}$ | | | 3.8×10^{-4} |
| $\bar{B}^0 \rightarrow \Delta^{++}\bar{\Delta}^{--}$ | | | 1.1×10^{-4} |
| $\bar{B}^0 \rightarrow \Delta^0\bar{\Delta}^0$ | | | 1.5×10^{-3} |

A. Experimental status

A.1. Two-body decays

The experimental results for two-body baryonic B decays are summarized in Tables I and II for charmless and charmful decays, respectively. It is clear that the present limit on charmless ones has been pushed to the level of 10^{-7} . In contrast, four of the charmful 2-body baryonic B decays have been observed in recent years; among them $\bar{B}^0 \rightarrow \Lambda_c^+\bar{p}$ is the first observation of

¹ In charm decay, $D_s^+ \rightarrow p\bar{n}$ is the only baryonic D decay mode which is physically allowed. However, its branching ratio is expected to be very small, of order 10^{-6} , because of partial conservation of axial current [1].

TABLE II: Branching ratios (in units of 10^{-5}) of charmful two-body baryonic B decays.

| Decay | Belle [14, 15, 16] | CLEO [17] |
|--|--|-----------|
| $\bar{B}^0 \rightarrow \Lambda_c^+ \bar{p}$ | $2.19_{-0.49}^{+0.56} \pm 0.32 \pm 0.57$ | < 9 |
| $B^- \rightarrow \Lambda_c^+ \bar{\Delta}^{--}$ | $0.65_{-0.51}^{+0.56} \pm 0.06 \pm 0.17 (< 1.9)$ | |
| $B^- \rightarrow \Lambda_c^+ \bar{\Delta}_X(1600)^{--}$ | $5.90_{-0.96}^{+1.03} \pm 0.55 \pm 1.53$ | |
| $B^- \rightarrow \Lambda_c^+ \bar{\Delta}_X(2420)^{--}$ | $4.70_{-0.92}^{+1.00} \pm 0.43 \pm 1.22$ | |
| $\bar{B}^0 \rightarrow \Lambda_c(2593)^- / \Lambda_c(2625)^- \bar{p}$ | | < 11 |
| $B^- \rightarrow \Sigma_c^0 \bar{p}$ | $3.67_{-0.66}^{+0.74} \pm 0.36 \pm 0.95$ | < 8 |
| $B^- \rightarrow \Sigma_c(2520)^0 \bar{p}$ | $1.26_{-0.49}^{+0.56} \pm 0.12 \pm 0.33 (< 2.7)$ | |
| $B^- \rightarrow \Xi_c^0(\rightarrow \Xi^- \pi^+) \bar{\Lambda}_c^-$ | $4.8_{-0.9}^{+1.0} \pm 1.1 \pm 1.2$ | |
| $\bar{B}^0 \rightarrow \Xi_c^+(\rightarrow \Xi^- \pi^+ \pi^+) \bar{\Lambda}_c^-$ | $9.3_{-2.8}^{+3.7} \pm 1.9 \pm 2.4$ | |

the 2-body baryonic B decay mode [15]. The decays with two charmed baryons in the final state were measured by Belle recently [16]. Taking the theoretical estimates (see e.g. Table III of [18]), $\mathcal{B}(\Xi_c^0 \rightarrow \Xi^- \pi^+) \approx 1.3\%$ and $\mathcal{B}(\Xi_c^+ \rightarrow \Xi^0 \pi^+) \approx 3.9\%$ together with the experimental measurement $\mathcal{B}(\Xi_c^+ \rightarrow \Xi^0 \pi^+) / \mathcal{B}(\Xi_c^+ \rightarrow \Xi^- \pi^+ \pi^+) = 0.55 \pm 0.16$ [19], it follows that

$$\mathcal{B}(B^- \rightarrow \Xi_c^0 \bar{\Lambda}_c^-) \approx 4.8 \times 10^{-3}, \quad \mathcal{B}(\bar{B}^0 \rightarrow \Xi_c^+ \bar{\Lambda}_c^-) \approx 1.2 \times 10^{-3}. \quad (1.1)$$

Therefore, the two-body doubly charmed baryonic B decay $B \rightarrow \mathcal{B}_c \bar{\mathcal{B}}'_c$ has a branching ratio of order 10^{-3} . Hence, we have the pattern

$$\mathcal{B}_c \bar{\mathcal{B}}'_c (\sim 10^{-3}) \gg \mathcal{B}_c \bar{\mathcal{B}} (\sim 10^{-5}) \gg \mathcal{B}_1 \bar{\mathcal{B}}_2 (\lesssim 10^{-7}) \quad (1.2)$$

for two-body baryonic B decays.

A.2. Three-body decays

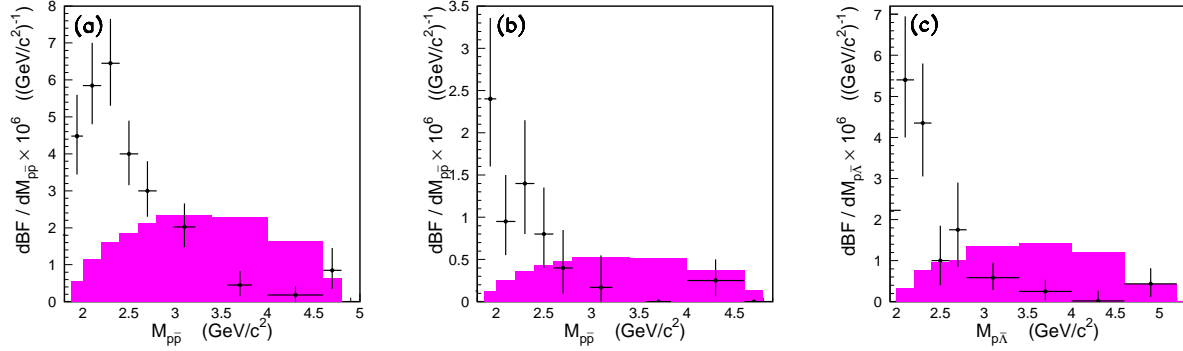
The measurements of three-body or four-body baryonic B decays are quite fruitful and many new results have been emerged in the past years. For the charmless case, Belle [20] has observed 6 different modes while BaBar has measured one of them, see Table III. The channel $B^- \rightarrow p \bar{p} K^-$ announced by Belle nearly four years ago [22] is the first observation of charmless baryonic B decays. Recently Belle has studied the baryon angular distribution in the baryon-antibaryon pair rest frame [21], while BaBar has measured the Dalitz plot asymmetry in the decay $B^- \rightarrow p \bar{p} K^-$. These measurements provide valuable information on the decay dynamics, as we shall discuss later.

Table IV summarizes the measured branching ratios of charmful baryonic decays with one charmed meson or one charmed baryon or two charmed baryons in the final state. In general, Belle results are slightly smaller than the CLEO measurements. The decay $B^- \rightarrow J/\psi \Lambda \bar{p}$ was first measured by BaBar [24] and an observation of this mode was made by Belle recently [28]. We see that $\mathcal{B}(B \rightarrow \mathcal{B}_c \bar{\mathcal{B}}'_c M) \sim \mathcal{O}(10^{-3})$ and $\mathcal{B}(B \rightarrow \mathcal{B}_c \bar{\mathcal{B}} M) \sim \mathcal{O}(10^{-4})$. The decay $B \rightarrow J/\psi \Lambda \bar{p}$ with the branching ratio of order 10^{-5} is suppressed due to color suppression.

There are two common and unique features for three-body $B \rightarrow \mathcal{B}_1 \bar{\mathcal{B}}_2 M$ decays: (i) The baryon-antibaryon invariant mass spectrum is peaked near the threshold area (see Fig. 1), and (ii) many three-body final states have rates larger than their two-body counterparts; that is, $\Gamma(B \rightarrow \mathcal{B}_1 \bar{\mathcal{B}}_2 M) > \Gamma(B \rightarrow \mathcal{B}_1 \bar{\mathcal{B}}_2)$. The low-mass enhancement effect indicates that the B meson is preferred to decay into a baryon-antibaryon pair with low invariant mass accompanied by

TABLE III: Branching ratios (in units of 10^{-6}) of charmless three-body baryonic B decays.

| Mode | BaBar [11] | Belle [20, 21] |
|--|-----------------------|-----------------------------------|
| $B^- \rightarrow p\bar{p}K^-$ | $6.7 \pm 0.5 \pm 0.4$ | $5.30^{+0.45}_{-0.39} \pm 0.58$ |
| $\bar{B}^0 \rightarrow p\bar{p}\bar{K}^0$ | | $1.20^{+0.32}_{-0.22} \pm 0.14$ |
| $B^- \rightarrow p\bar{p}K^{*-}$ | | $10.31^{+3.62+1.34}_{-2.77-1.65}$ |
| $B^- \rightarrow p\bar{p}\pi^-$ | | $3.06^{+0.73}_{-0.62} \pm 0.37$ |
| $\bar{B}^0 \rightarrow \Lambda\bar{p}\pi^+$ | | $3.27^{+0.62}_{-0.51} \pm 0.39$ |
| $B^- \rightarrow \Lambda\bar{\Lambda}K^-$ | | $2.91^{+0.90}_{-0.70} \pm 0.38$ |
| $B^- \rightarrow \Lambda\bar{\Lambda}\pi^-$ | | < 2.8 |
| $\bar{B}^0 \rightarrow p\bar{p}\bar{K}^{*0}$ | | < 7.6 |
| $\bar{B}^0 \rightarrow \Lambda\bar{p}K^+$ | | < 0.82 |
| $\bar{B}^0 \rightarrow \Sigma^0\bar{p}\pi^+$ | | < 3.8 |


 FIG. 1: Invariant mass distributions for (a) $p\bar{p}K^+$, (b) $p\bar{p}K_S^0$, and (c) $p\bar{\Lambda}\pi^-$. The shaded distribution shows the expectation from a phase-space MC simulation with area scaled to the signal yield [21].

a fast recoil meson. As for the above-mentioned second feature, it is by now well established experimentally that

$$\begin{aligned}
 \mathcal{B}(B^- \rightarrow p\bar{p}K^-) &\gg \mathcal{B}(\bar{B}^0 \rightarrow p\bar{p}), & \mathcal{B}(\bar{B}^0 \rightarrow \Lambda\bar{p}\pi^-) &\gg \mathcal{B}(B^- \rightarrow \Lambda\bar{p}), \\
 \mathcal{B}(B^- \rightarrow \Lambda_c^+\bar{p}\pi^-) &\gg \mathcal{B}(\bar{B}^0 \rightarrow \Lambda_c^+\bar{p}), & \mathcal{B}(B^- \rightarrow \Sigma_c^0\bar{p}\pi^0) &\gg \mathcal{B}(B^- \rightarrow \Sigma_c^0\bar{p}).
 \end{aligned} \quad (1.3)$$

This phenomenon can be understood in terms of the threshold effect, namely, the invariant mass of the dibaryon is preferred to be close to the threshold. The configuration of the two-body decay $B \rightarrow \mathcal{B}_1\bar{\mathcal{B}}_2$ is not favorable since its invariant mass is m_B . In $B \rightarrow \mathcal{B}_1\bar{\mathcal{B}}_2M$ decays, the effective mass of the baryon pair is reduced as the emitted meson can carry away much energies.

An enhancement of the dibaryon invariant mass near threshold has been observed in the charmless decays $\bar{B}^0 \rightarrow \Lambda\bar{p}\pi^+$, $\bar{B}^0 \rightarrow p\bar{p}K_S$, $B^- \rightarrow p\bar{p}K^-$, $B^- \rightarrow p\bar{p}\pi^-$, $B^- \rightarrow \Lambda\bar{\Lambda}K^-$ [11, 20, 21], and in the charmful decays $B^- \rightarrow \Lambda_c^+\bar{p}\pi^-$, $\bar{B}^0 \rightarrow p\bar{p}D^0$ and $\bar{B}^0 \rightarrow p\bar{p}D^{*0}$ [14, 23, 25]. The same threshold behavior has also been observed in the baryonic J/ψ decays: $J/\psi \rightarrow \gamma p\bar{p}$ and $J/\psi \rightarrow K^-p\bar{\Lambda}$ [30, 31]. However, no low-mass enhancement effect is seen in the charmful decays $\bar{B}^0 \rightarrow \Sigma_c(2455)^{++}\bar{p}\pi^-$,

TABLE IV: Experimental measurements of the branching ratios (in units of 10^{-4}) for the B decay modes with a charmed baryon $\Lambda_c(2285)$ or $\Lambda_{c1} = \Lambda_c(2593)/\Lambda_c(2625)$ or $\Sigma_c(2455)$ or $\Sigma_{c1} = \Sigma_c(2520)$ or a charmed meson in the final state.

| Mode | BaBar [23, 24] | Belle [14, 25, 26, 27, 28] | CLEO [17, 29] |
|---|---|---|---------------------------------------|
| $\bar{B}^0 \rightarrow D^{*+} p \bar{p} \pi^-$ | $5.61 \pm 0.59 \pm 0.73$ | | $6.5^{+1.3}_{-1.2} \pm 1.0$ |
| $\bar{B}^0 \rightarrow D^+ p \bar{p} \pi^-$ | $3.80 \pm 0.35 \pm 0.46$ | | |
| $\bar{B}^0 \rightarrow D^{*+} n \bar{p}$ | | | $14.5^{+3.4}_{-3.0} \pm 2.7$ |
| $\bar{B}^0 \rightarrow D^0 p \bar{p}$ | $1.24 \pm 0.14 \pm 0.12$ | $1.18 \pm 0.15 \pm 0.16$ | |
| $\bar{B}^0 \rightarrow D^{*0} p \bar{p}$ | $0.67 \pm 0.21 \pm 0.09$ | $1.20^{+0.33}_{-0.29} \pm 0.21$ | |
| $B^- \rightarrow D^- p \bar{p}$ | | < 0.15 | |
| $B^- \rightarrow D^{*-} p \bar{p}$ | | < 0.15 | |
| $B^- \rightarrow J/\psi \Lambda \bar{p}$ | $(11.6^{+7.4+4.2}_{-5.3-1.8}) \times 10^{-2}$ | $(11.6 \pm 2.8^{+1.8}_{-2.3}) \times 10^{-2}$ | |
| $B^- \rightarrow J/\psi \Sigma^0 \bar{p}$ | | < 0.11 | |
| $\bar{B}^0 \rightarrow J/\psi p \bar{p}$ | | $< 8.3 \times 10^{-3}$ | |
| $B^- \rightarrow \Lambda_c^+ \bar{p} \pi^- \pi^+ \pi^-$ | | | $22.5 \pm 2.5^{+2.4}_{-1.9} \pm 5.8$ |
| $B^- \rightarrow \Lambda_c^+ \bar{p} \pi^- \pi^0$ | | $11.0 \pm 1.2 \pm 1.9 \pm 2.9$ | $18.1 \pm 2.9^{+2.2}_{-1.6} \pm 4.7$ |
| $\bar{B}^0 \rightarrow \Lambda_c^+ \bar{p} \pi^+ \pi^-$ | | $10.3 \pm 0.9 \pm 1.2 \pm 2.7$ | $16.7 \pm 1.9^{+1.9}_{-1.6} \pm 4.3$ |
| $B^- \rightarrow \Lambda_c^+ \bar{p} \pi^-$ | | $2.01 \pm 0.15 \pm 0.20 \pm 0.52$ | $2.4 \pm 0.6^{+0.19}_{-0.17} \pm 0.6$ |
| $B^- \rightarrow \Lambda_{c1}^+ \bar{p} \pi^-$ | | | < 1.9 |
| $B^- \rightarrow \Sigma_c^{++} \bar{p} \pi^- \pi^-$ | | | $2.8 \pm 0.9 \pm 0.5 \pm 0.7$ |
| $B^- \rightarrow \Sigma_c^0 \bar{p} \pi^+ \pi^-$ | | | $4.4 \pm 1.2 \pm 0.5 \pm 1.1$ |
| $\bar{B}^0 \rightarrow \Sigma_c^{++} \bar{p} \pi^-$ | | $1.15 \pm 0.22 \pm 0.14 \pm 0.30$ | $3.7 \pm 0.8 \pm 0.7 \pm 1.0$ |
| $\bar{B}^0 \rightarrow \Sigma_c^0 \bar{p} \pi^+$ | | $0.97 \pm 0.21 \pm 0.12 \pm 0.25$ | $2.2 \pm 0.6 \pm 0.4 \pm 0.6$ |
| $B^- \rightarrow \Sigma_c^0 \bar{p} \pi^0$ | | | $4.2 \pm 1.3 \pm 0.4 \pm 1.1$ |
| $\bar{B}^0 \rightarrow \Sigma_{c1}^{++} \bar{p} \pi^-$ | | $1.04 \pm 0.24 \pm 0.12 \pm 0.27$ | |
| $\bar{B}^0 \rightarrow \Sigma_{c1}^0 \bar{p} \pi^+$ | | $0.33 \pm 0.19 \pm 0.04 \pm 0.09$ | |
| $B^- \rightarrow \Lambda_c^+ \bar{\Lambda}_c^- K^-$ | | $6.5^{+1.0}_{-0.9} \pm 1.1 \pm 3.4$ | |
| $\bar{B}^0 \rightarrow \Lambda_c^+ \bar{\Lambda}_c^- \bar{K}^0$ | | $7.9^{+2.9}_{-2.3} \pm 1.2 \pm 4.1$ | |

$\Sigma_c(2455)^0 \bar{p} \pi^+$ [26] and $B^- \rightarrow J/\psi \Lambda \bar{p}$ [28].

Threshold enhancement was first conjectured by Hou and Soni [32], motivated by the CLEO measurement of $B \rightarrow D^* p \bar{n}$ and $D^* p \bar{p} \pi$ [29]. They argued that in order to have larger baryonic B decays, one has to reduce the energy release and at the same time allow for baryonic ingredients to be present in the final state. This is indeed the near threshold effect mentioned above. Of course, one has to understand the underlying origin of the threshold peaking effect. Hence, the smallness of the two-body baryonic decay $B \rightarrow \mathcal{B}_1 \bar{\mathcal{B}}_2$ has to do with its large energy release.

Note that the invariant mass distributions for $J/\psi \rightarrow \gamma p \bar{p}$ and $B^- \rightarrow \Lambda_c^+ \bar{p} \pi^-$ are so sharply peaked near threshold that they can be interpreted as some Breit-Wigner resonances:² $M =$

² There is a difference between the threshold effects observed in $J/\psi \rightarrow \gamma p \bar{p}$ and $B^- \rightarrow p \bar{p} K^-$ decays. The spectrum for the latter (see Fig. 1) is peaked near the threshold, but not really at threshold, and is much

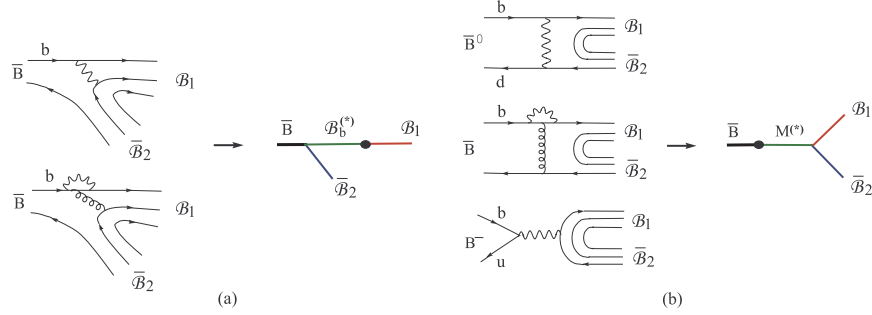


FIG. 2: Quark and pole diagrams for two-body baryonic B decay $\bar{B} \rightarrow \mathcal{B}_1 \bar{\mathcal{B}}_2$, where the symbol \bullet denotes the weak vertex.

(1859^{+3+5}_{-10-25}) MeV and $\Gamma < 30$ MeV for the former [30] and $M = (3.35^{+0.01}_{-0.02} \pm 0.02)$ GeV and $\Gamma = (70^{+40}_{-30} \pm 40)$ MeV for the latter [14]. A popular interpretation of the $p\bar{p}$ threshold enhancement observed in $J/\psi \rightarrow \gamma p\bar{p}$ is to postulate the existence of a $p\bar{p}$ bound state, known as baryonium. Indeed, a new resonance $X(1835)$ was recently observed by BES in the $\pi^+\pi^-\eta'$ invariant mass [33]. It has a mass $M = 1833.7 \pm 6.1 \pm 2.7$ MeV and a width $\Gamma = 67.7 \pm 20.3 \pm 7.7$ MeV. As for the low $p\bar{p}$ mass enhancement observed in B decays, it has been suggested that a possible glueball resonance with a mass near 2.3 GeV may contribute to the threshold enhancement behavior for the $p\bar{p}K^-$ mode [34]. Although this possibility is ruled out experimentally [21], a gluonic resonant state near or below the $p\bar{p}$ threshold still remains plausible. For decays such as $\bar{B}^0 \rightarrow \Lambda \bar{p} \pi^+$, $\bar{B}^0 \rightarrow D^0 p \bar{p}$ and $B^- \rightarrow p \bar{p} \pi^-$, the threshold phenomenon cannot be accounted for by the intermediate gluonic effects. In this case, low mass enhancement should be explained in terms of the usual heavy decay process (or the so-called fragmentation process in [35]).

B. Theoretical progress

Since baryonic B decays involve two baryons, it is extremely complicated and much involved. Nevertheless, there are some theoretical progresses in the past five years.

It is known that two-body baryonic B decays are dominated by nonfactorizable contributions that are difficult to evaluate. This nonfactorizable effect can be evaluated in the pole model. Using the MIT bag model to evaluate the weak matrix elements and the 3P_1 model to estimate the strong coupling constants, it is found in [36] and [37] that the charmless and charmful two-body decays can be well described. Chang and Hou [38] have generalized the original version of the diquark model [8] to include penguin effects, though no quantitative predictions are made. In the meantime, a diagrammatic approach has been developed for both charmful [39] and charmless [40] decays. A different approach for analyzing the helicity structure of the charmless two-body baryonic decays is performed in [41] with results similar to [40].

Contrary to the two-body baryonic B decay, the three-body decays do receive factorizable

wider than that in J/ψ decays. Hence, it is often argued that threshold enhancement in $J/\psi \rightarrow \gamma p\bar{p}$ cannot be explained in terms of the heavy quark decay process. Nevertheless, it will be interesting to see if the threshold effects observed in $J/\psi \rightarrow \gamma p\bar{p}$ and $B^- \rightarrow p\bar{p}X$ ($X = K^-, \pi^-$) decays share the same origin.

contributions that fall into two categories: (i) the transition process with a meson emission, $\langle M | (\bar{q}_3 q_2) | 0 \rangle \langle \mathcal{B}_1 \bar{\mathcal{B}}_2 | (\bar{q}_1 b) | B \rangle$, and (ii) the current-induced process governed by the factorizable amplitude $\langle \mathcal{B}_1 \bar{\mathcal{B}}_2 | (\bar{q}_1 q_2) | 0 \rangle \langle M | (\bar{q}_3 b) | B \rangle$. The two-body matrix element $\langle \mathcal{B}_1 \bar{\mathcal{B}}_2 | (\bar{q}_1 q_2) | 0 \rangle$ in the latter process can be either related to some measurable quantities or calculated using the quark model. The current-induced contribution to three-body baryonic B decays has been discussed in various publications [42, 43, 44]. On the contrary, it is difficult to evaluate the three-body matrix element in the transition process and in this case one can appeal to the pole model [36, 37, 45].

Weak radiative baryonic B decays $B \rightarrow \mathcal{B}_1 \bar{\mathcal{B}}_2 \gamma$ mediated by the electromagnetic penguin process $b \rightarrow s \gamma$ may have appreciable rates. Based on the pole model, it is found that $B^- \rightarrow \Lambda \bar{p} \gamma$ and $B^- \rightarrow \Xi^0 \bar{\Sigma}^- \gamma$ have sizable rates and are readily accessible to B factories [46].

II. 2-BODY BARYONIC B DECAYS

As shown in Fig. 2, the quark diagrams for two-body baryonic B decays consist of internal W -emission diagram, $b \rightarrow d(s)$ penguin transition, W -exchange for the neutral B meson and W -annihilation for the charged B . Just as mesonic B decays, W -exchange and W -annihilation are expected to be helicity suppressed. Therefore, the two-body baryonic B decay $B \rightarrow \mathcal{B}_1 \bar{\mathcal{B}}_2$ receives the main contributions from the internal W -emission diagram for tree-dominated modes and the penguin diagram for penguin-dominated processes. It should be stressed that, contrary to mesonic B decays, internal W emission in baryonic B decays is not necessarily color suppressed. This is because the baryon wave function is totally antisymmetric in color indices. One can see from Fig. 2 that there is no color suppression for the meson production. In the effective Hamiltonian approach, the relevant four-quark operators are $O_1 = (\bar{s}q)(\bar{q}b)$ and $O_2 = (\bar{q}q)(\bar{s}b)$. The combination of the operators $O_1 - O_2$ is antisymmetric in color indices (more precisely, it is a color sextet). Therefore, the Wilson coefficient for tree-dominated internal W -emission would be $c_1 - c_2$ rather than $a_2 = c_2 + c_1/3$. This is indeed the case found in the pole model calculation in [36].

From the previous argument that one has to reduce the energy release in order to have larger baryonic B decays [32], it is expected that

$$\Gamma(B \rightarrow \mathcal{B}_1 \bar{\mathcal{B}}_2) = |\text{CKM}|^2 / f(\text{energy release}), \quad (2.1)$$

where CKM stands for the relevant CKM angles. For charmful modes, the CKM angles for $\Xi_c \bar{\Lambda}_c$ and $\Lambda_c \bar{p}$ have the same magnitudes except for a sign difference. Therefore, one will expect

$$\mathcal{B}(\bar{B}^0 \rightarrow \Lambda_c^+ \bar{p}) = \mathcal{B}(\bar{B}^0 \rightarrow \Xi_c^+ \bar{\Lambda}_c)(\text{dynamical suppression}). \quad (2.2)$$

where the dynamical suppression arises from the larger energy release in $\Lambda_c^+ \bar{p}$ than in $\Xi_c \bar{\Lambda}_c$. Eq. (1.2) implies that the dynamical suppression effect is of order 10^{-2} . Likewise,

$$\begin{aligned} \mathcal{B}(B^- \rightarrow \Lambda \bar{p}) &= \mathcal{B}(\bar{B}^0 \rightarrow \Lambda_c^+ \bar{p}) |V_{ub}/V_{cb}|^2 (\text{dynamical suppression})' \\ &\sim 2 \times 10^{-7} (\text{dynamical suppression})'. \end{aligned} \quad (2.3)$$

If the dynamical suppression of $\Lambda \bar{p}$ relative to $\Lambda_c \bar{p}$ is similar to that of $\Lambda_c \bar{p}$ relative to $\Xi_c \bar{\Lambda}_c$, the branching ratio of the charmless two-body baryonic B decays can be even as small as 10^{-9} . If it is the case, then it will be hopeless to see any charmless two-body baryonic B decays.

Since $B \rightarrow \mathcal{B}_1 \bar{\mathcal{B}}_2$ amplitudes are nonfactorizable in nature, it is very difficult to evaluate them directly. In order to circumvent this difficulty, it is customary to assume that the decay amplitude

at the hadron level is dominated by the pole diagrams with low-lying one-particle intermediate states. The general amplitude reads

$$\mathcal{A}(B \rightarrow \mathcal{B}_1 \bar{\mathcal{B}}_2) = \bar{u}_1(A + B\gamma_5)v_2, \quad (2.4)$$

where A and B correspond to p -wave parity-violating (PV) and s -wave parity-conserving (PC) amplitudes, respectively. In the pole model, PC and PV amplitudes are dominated by $\frac{1}{2}^+$ ground-state intermediate states and $\frac{1}{2}^-$ low-lying baryon resonances, respectively. This pole model has been applied successfully to nonleptonic decays of hyperons and charmed baryons [18, 47]. In general, the pole diagram leads to

$$A = - \sum_{\mathcal{B}_b^*} \frac{g_{\mathcal{B}_b^* \rightarrow B \mathcal{B}_2} b_{\mathcal{B}_b^* \mathcal{B}_1}}{m_1 - m_{\mathcal{B}_b^*}}, \quad B = \sum_{\mathcal{B}_b} \frac{g_{\mathcal{B}_b \rightarrow B \mathcal{B}_2} a_{\mathcal{B}_b \mathcal{B}_1}}{m_1 - m_{\mathcal{B}_b}}. \quad (2.5)$$

There are two unknown quantities in the above equation: weak matrix elements and strong couplings. For the former one can employ the MIT bag model to evaluate the baryon-to-baryon transitions [36]. For the latter, there are two distinct models for quark pair creation: (i) the 3P_0 model in which the $q\bar{q}$ pair is created from the vacuum with vacuum quantum numbers. Presumably it works in the nonperturbative low energy regime, and (ii) the 3S_1 model in which the quark pair is created perturbatively via one gluon exchange with one-gluon quantum numbers 3S_1 . Since the light baryons produced in two-body baryonic B decays are very energetic, it appears that the 3S_1 model may be more relevant for charmless decays. It is not difficult to see from Fig. 2(a) that one needs to attach two hard gluons for charmless and singly charmful 2-body baryonic B decays.

From Table V we see that the charmless two-body baryonic decays are predicted at the level of 10^{-7} . This may indicate that the dynamical suppression of $\mathcal{B}_1 \bar{\mathcal{B}}_2$ relative to $\mathcal{B}_c \bar{\mathcal{B}}$ is not significant. The predictions for charmful $B \rightarrow \mathcal{B}_c \bar{\mathcal{B}}$ decays are summarized in Table VI. All earlier predictions based on the sum-rule analysis, the pole model and the diquark model are too large compared to experiment. Note that we predict that $B^- \rightarrow \Sigma_c^0 \bar{p}$ has a larger rate than $\bar{B}^0 \rightarrow \Lambda_c \bar{p}$ since the former proceeds via the Λ_b pole while the latter via the Σ_b pole and the $\Lambda_b N \bar{B}$ coupling is larger than the $\Sigma_b N \bar{B}$ one [37].

Since the doubly charmed baryonic decay mode $\Xi_c \bar{\Lambda}_c$ proceeds via $b \rightarrow cs\bar{c}$, while $\Lambda_c \bar{p}$ via a $b \rightarrow cd\bar{u}$ quark transition, the CKM mixing angles for them are the same in magnitude but opposite in sign, one may wonder why the $\mathcal{B}_c \bar{\mathcal{B}}'_c$ mode has a rate two orders of magnitude larger than $\mathcal{B}_c \bar{\mathcal{B}}$. Indeed, earlier calculations based on QCD sum rules [7] or the diquark model [8] all predict that $\mathcal{B}(B \rightarrow \Xi_c \bar{\Lambda}_c) \approx \mathcal{B}(\bar{B} \rightarrow \mathcal{B}_c \bar{N})$, which is in strong disagreement with experiment. This implies that some important dynamical suppression effect for the $\mathcal{B}_c \bar{N}$ production with respect to $\Xi_c \bar{\Lambda}_c$ is missing in previous studies. Recently, this issue was investigated in [48]. Since the energy release is relatively small in charmful baryonic B decay, the 3P_0 model for $q\bar{q}$ production is more relevant. In the work of [48], the possibility that the $q\bar{q}$ pair produced via light meson exchanges such as σ and pions is considered. The $q\bar{q}$ pair created from soft nonperturbative interactions tends to be soft. For an energetic proton produced in 2-body B decays, the momentum fraction carried by its quark is large, $\sim \mathcal{O}(1)$, while for an energetic charmed baryon, its momentum is carried mostly by the charmed quark. As a consequence, the doubly charmed baryon state such as $\Xi_c \bar{\Lambda}_c$ has a configuration more favorable than $\Lambda_c \bar{p}$.

Assuming that a soft $q\bar{q}$ quark pair is produced through the σ and π meson exchanges in the configuration for $\bar{B} \rightarrow \Xi_c \bar{\Lambda}_c$, it is found that its branching ratio is of order 10^{-3} (see [48] for detail), in agreement with experiment. Note that this calculation is not applicable to the two-body decay

TABLE V: Predictions of the branching ratios for some charmless two-body baryonic B decays classified into two categories: tree-dominated and penguin-dominated. Branching ratios denoted by “†” are calculated only for the parity-conserving part. Experimental limits are taken from Table I.

| | [7] | [6] | [36] | Expt. |
|--|-----------------------------|----------------------|-----------------------------|------------------------|
| $\bar{B}^0 \rightarrow p\bar{p}$ | 1.2×10^{-6} | 7.0×10^{-6} | $1.1 \times 10^{-7\dagger}$ | $< 2.7 \times 10^{-7}$ |
| $\bar{B}^0 \rightarrow n\bar{n}$ | 3.5×10^{-7} | 7.0×10^{-6} | $1.2 \times 10^{-7\dagger}$ | |
| $B^- \rightarrow n\bar{p}$ | 6.9×10^{-7} | 1.7×10^{-5} | 5.0×10^{-7} | |
| $\bar{B}^0 \rightarrow \Lambda\bar{\Lambda}$ | | 2×10^{-7} | 0^\dagger | $< 6.9 \times 10^{-7}$ |
| $B^- \rightarrow p\bar{\Delta}^{--}$ | 2.9×10^{-7} | 3.2×10^{-4} | 1.4×10^{-6} | $< 1.5 \times 10^{-4}$ |
| $\bar{B}^0 \rightarrow p\bar{\Delta}^-$ | 7×10^{-8} | 1.0×10^{-4} | 4.3×10^{-7} | |
| $B^- \rightarrow n\bar{\Delta}^-$ | | 1×10^{-7} | 4.6×10^{-7} | |
| $\bar{B}^0 \rightarrow n\bar{\Delta}^0$ | | 1.0×10^{-4} | 4.3×10^{-7} | |
| $B^- \rightarrow \Lambda\bar{p}$ | $\lesssim 3 \times 10^{-6}$ | | $2.2 \times 10^{-7\dagger}$ | $< 4.9 \times 10^{-7}$ |
| $\bar{B}^0 \rightarrow \Lambda\bar{n}$ | | | $2.1 \times 10^{-7\dagger}$ | |
| $\bar{B}^0 \rightarrow \Sigma^+\bar{p}$ | 6×10^{-6} | | $1.8 \times 10^{-8\dagger}$ | |
| $B^- \rightarrow \Sigma^0\bar{p}$ | 3×10^{-6} | | $5.8 \times 10^{-8\dagger}$ | |
| $B^- \rightarrow \Sigma^+\bar{\Delta}^{--}$ | 6×10^{-6} | | 2.0×10^{-7} | |
| $\bar{B}^0 \rightarrow \Sigma^+\bar{\Delta}^-$ | 6×10^{-6} | | 6.3×10^{-8} | |
| $B^- \rightarrow \Sigma^-\bar{\Delta}^0$ | 2×10^{-6} | | 8.7×10^{-8} | |

TABLE VI: Predictions of charmful two-body baryonic B decays. Experimental results are taken from Table II.

| | [6] | [37] | Expt. |
|--|----------------------|----------------------|---|
| $\bar{B}^0 \rightarrow \Lambda_c^+\bar{p}$ | 1.1×10^{-3} | 1.1×10^{-5} | $(2.19 \pm 0.84) \times 10^{-5}$ |
| $B^- \rightarrow \Sigma_c^0\bar{p}$ | 1.5×10^{-2} | 6.0×10^{-5} | $(3.67^{+0.74}_{-0.66} \pm 1.01) \times 10^{-5}$ |
| $\bar{B}^0 \rightarrow \Sigma_c^0\bar{n}$ | 5.8×10^{-3} | 6.0×10^{-7} | |
| $B^- \rightarrow \Lambda_c^+\bar{\Delta}^{--}$ | 3.6×10^{-2} | 1.9×10^{-5} | $(0.65^{+0.56}_{-0.51} \pm 0.18) \times 10^{-5} (< 1.9 \times 10^{-5})$ |

$\bar{B}^0 \rightarrow \Lambda_c^+\bar{p}$ with one charmed baryon in the final state. This is because two hard gluons are needed to produce an energetic antiproton as noticed before: one hard gluon for kicking the spectator quark of the B meson to make it energetic and the other for producing the hard $q\bar{q}$ pair. The pQCD calculation for this decay will be much more involved (see e.g. [51] for pQCD calculations of $\Lambda_b \rightarrow \Lambda J/\psi$). Nevertheless, it is expected that $\Gamma(\bar{B} \rightarrow \mathcal{B}_c \bar{N}) \ll \Gamma(\bar{B} \rightarrow \Xi_c \bar{\Lambda}_c)$ as the former is suppressed by order of α_s^4 . This dynamical suppression effect for the $\Lambda_c \bar{p}$ production relative to $\Xi_c \bar{\Lambda}_c$ has been neglected in the previous studies based on QCD sum rules [7] and on the diquark model [8].

TABLE VII: Predictions on the branching ratios of $B^- \rightarrow \Xi_c^0 \bar{\Lambda}_c^-$ and $\bar{B}^0 \rightarrow \Xi_c^+ \bar{\Lambda}_c^-$ decays [48]. The first and second errors come from the theoretical uncertainties in the parameters β and ω_b , respectively, which are taken to be $\beta = 1.20 \pm 0.05$ GeV and $\omega_b = 0.45 \pm 0.05$ GeV. Results shown in second and third rows are from π or σ exchange alone, respectively.

| Mode | Theory (10^{-3}) | Expt (10^{-3}) | Mode | Theory (10^{-3}) | Expt (10^{-3}) |
|---|-----------------------------|--------------------|---|-----------------------------|--------------------|
| $\mathcal{B}(B^- \rightarrow \Xi_c^0 \bar{\Lambda}_c^-)$ | $1.0^{+0.3+1.1}_{-0.3-0.7}$ | ≈ 4.8 | $\mathcal{B}(\bar{B}^0 \rightarrow \Xi_c^+ \bar{\Lambda}_c^-)$ | $0.9^{+0.2+1.0}_{-0.3-0.6}$ | ≈ 1.2 |
| $\mathcal{B}(B^- \rightarrow \Xi_c^0 \bar{\Lambda}_c^-)_\pi$ | $0.8^{+0.2+0.9}_{-0.2-0.6}$ | | $\mathcal{B}(\bar{B}^0 \rightarrow \Xi_c^+ \bar{\Lambda}_c^-)_\pi$ | $0.8^{+0.2+0.8}_{-0.2-0.5}$ | |
| $\mathcal{B}(B^- \rightarrow \Xi_c^0 \bar{\Lambda}_c^-)_\sigma$ | $0.1^{+0.0+0.1}_{-0.0-0.1}$ | | $\mathcal{B}(\bar{B}^0 \rightarrow \Xi_c^+ \bar{\Lambda}_c^-)_\sigma$ | $0.1^{+0.0+0.1}_{-0.0-0.1}$ | |

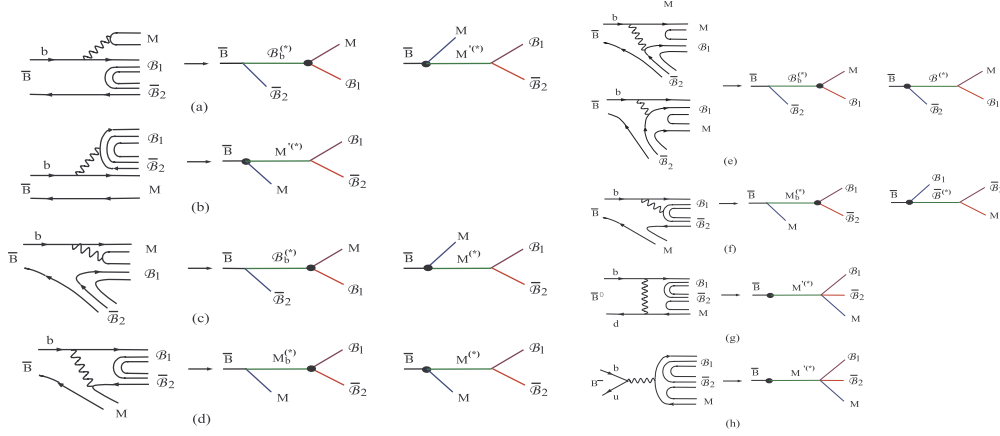


FIG. 3: Quark and pole diagrams for three-body baryonic B decay $\bar{B} \rightarrow \mathcal{B}_1 \bar{\mathcal{B}}_2 M$, where the symbol \bullet denotes the weak vertex.

III. 3-BODY BARYONIC B DECAYS

In three-body baryonic B decays, the emission of the meson M can carry away energies in such a way that the invariant mass of $\mathcal{B}_1 \bar{\mathcal{B}}_2$ becomes smaller and hence it is relatively easier to fragment into the baryon-antibaryon pair. One can also understand this feature more concretely by studying the Dalitz plot. Due to the $V-A$ nature of the $b \rightarrow u\bar{d}$ process, the invariant mass of the diquark ud peaks at the highest possible values in a Dalitz plot for $b \rightarrow u\bar{d}\bar{d}$ transition [52]. If the ud forms a nucleon, then the very massive udq objects will intend to form a highly excited baryon state such as Δ and N^* and will be seen as $Nn\pi$ ($n \geq 1$) [53]. This explains the non-observation of the $N\bar{N}$ final states and why the three-body mode $N\bar{N}\pi(\rho)$ is favored. Of course, this argument is applicable only to the tree-dominated processes.

The quark diagrams and the corresponding pole diagrams for decays of B mesons to the baryonic final state $\mathcal{B}_1 \bar{\mathcal{B}}_2 M$ are more complicated. In general, there are two external W -diagrams Figs. 3(a)-3(b), four internal W -emissions Figs. 3(c)-3(f), and one W -exchange Fig. 3(g) for the neutral B meson and one W -annihilation Fig. 3(h) for the charged B . For simplicity, penguin diagrams are not drawn in Fig. 3, but they can be obtained from Figs. 3(c)-3(g) by replacing the $b \rightarrow u$ tree transition by the $b \rightarrow s(d)$ penguin transition. Under the factorization hypothesis, the relevant

factorizable amplitudes are

$$\begin{aligned}
\text{Figs. 3(a), 3(c)} : \quad & A \propto \langle M | (\bar{q}_3 q_2) | 0 \rangle \langle \mathcal{B}_1 \bar{\mathcal{B}}_2 | (\bar{q}_1 b) | \bar{B} \rangle, \\
\text{Figs. 3(b), 3(d)} : \quad & A \propto \langle \mathcal{B}_1 \bar{\mathcal{B}}_2 | (\bar{q}_1 q_2) | 0 \rangle \langle M | (\bar{q}_3 b) | \bar{B} \rangle, \\
\text{Figs. 3(g), 3(h)} : \quad & A \propto \langle \mathcal{B}_1 \bar{\mathcal{B}}_2 M | (\bar{q}_1 q_2) | 0 \rangle \langle 0 | (\bar{q}_3 b) | \bar{B} \rangle.
\end{aligned} \tag{3.1}$$

Neglecting the factorizable annihilation contributions which are helicity suppressed, the three-body decays that receive factorizable contributions fall into two categories: (i) the transition process with a meson emission, $\langle M | (\bar{q}_3 q_2) | 0 \rangle \langle \mathcal{B}_1 \bar{\mathcal{B}}_2 | (\bar{q}_1 b) | \bar{B} \rangle$, and (ii) the current-induced process governed by the factorizable amplitude $\langle \mathcal{B}_1 \bar{\mathcal{B}}_2 | (\bar{q}_1 q_2) | 0 \rangle \langle M | (\bar{q}_3 b) | \bar{B} \rangle$. The two-body matrix element $\langle \mathcal{B}_1 \bar{\mathcal{B}}_2 | (\bar{q}_1 q_2) | 0 \rangle$ in the latter process can be either related to some measurable quantities or calculated using the quark model. The current-induced contribution to three-body baryonic B decays has been discussed in various publications [42, 43, 44]. On the contrary, it is difficult to evaluate the three-body matrix element in the transition process and in this case one can appeal to the pole model [36, 37, 45]. For Figs. 3(a) and 3(c) we will consider the pole diagrams to evaluate 3-body matrix elements. The 3-body matrix element $\langle \mathcal{B}_1 \bar{\mathcal{B}}_2 | (\bar{q}_1 b) | B \rangle$ receives contributions from point-like contact interaction (i.e. direct weak transition) and pole diagrams [36].

It should be stressed that among the four internal W -emission diagrams, Figs. 3(c) and 3(d) are color suppressed while Figs. 3(e) and 3(f) are not due to baryon wave function antisymmetric in color indices [37]. For example, $B \rightarrow J/\psi \Lambda \bar{p}$ proceeds via Fig. 3(c), while $B^- \rightarrow \Sigma_c^0 \bar{p} \pi^+$ receives the dominant contributions from Figs. 3(e) and 3(f). The experimental observation that $\Sigma_c^0 \bar{p} \pi^+$ has a rate similar to $\Sigma_c^{++} \bar{p} \pi^-$ which proceeds via external W -emission Fig. 3(a) and that $J/\psi \Lambda \bar{p}$ is suppressed by one order of magnitude implies the color suppression for Fig. 3(c) and non-suppression for Figs. 3(e) and 3(f).

A. Current-induced three-body baryonic B decays

Current-induced three-body baryonic B decays such as $\bar{B}^0 \rightarrow \Lambda \bar{p} \pi^+$ provide an ideal place for understanding the threshold enhancement effects. Theoretically, the low-mass enhancement effect is closely linked to the behavior of the baryon form factors occurred in the vacuum to $\mathcal{B}_1 \bar{\mathcal{B}}_2$ transition matrix element

$$\begin{aligned}
\langle \mathcal{B}_1(p_1) \bar{\mathcal{B}}_2(p_2) | (V \pm A)_\mu | 0 \rangle = & \bar{u}_1(p_1) \left\{ f_1^{\mathcal{B}_1 \mathcal{B}_2}(t) \gamma_\mu + i \frac{f_2^{\mathcal{B}_1 \mathcal{B}_2}(t)}{m_1 + m_2} \sigma_{\mu\nu} q^\nu + \frac{f_3^{\mathcal{B}_1 \mathcal{B}_2}(t)}{m_1 + m_2} q_\mu \right. \\
& \left. \pm \left[g_1^{\mathcal{B}_1 \mathcal{B}_2}(t) \gamma_\mu + i \frac{g_2^{\mathcal{B}_1 \mathcal{B}_2}(t)}{m_1 + m_2} \sigma_{\mu\nu} q^\nu + \frac{g_3^{\mathcal{B}_1 \mathcal{B}_2}(t)}{m_1 + m_2} q_\mu \right] \gamma_5 \right\} v_2(p_2), \tag{3.2}
\end{aligned}$$

where $t = (p_1 + p_2)^2 = M_{\mathcal{B}_1 \bar{\mathcal{B}}_2}^2$. The form factors $f_i^{\mathcal{B}_1 \mathcal{B}_2}(t)$ and $g_i^{\mathcal{B}_1 \mathcal{B}_2}(t)$ expressed in terms of a power series of the inverse of the dibaryon invariant mass squared $M_{\mathcal{B}_1 \bar{\mathcal{B}}_2}^2$ will fall off sharply with t . For octet baryons one can apply SU(3) symmetry to relate the vector form factors $f_i^{\mathcal{B}_1 \mathcal{B}_2}$ to the nucleon magnetic and electric form factors which have been measured over a large range of q^2 .

The decay $\bar{B}^0 \rightarrow \Lambda \bar{p} \pi^+$ receives the dominant factorizable contributions from the tree diagram Fig. 3(b) and the penguin diagram Fig. 3(d) with the amplitudes (see e.g. [36])

$$\begin{aligned}
A(\bar{B}^0 \rightarrow \Lambda \bar{p} \pi^+) = & \frac{G_F}{\sqrt{2}} \langle \pi^+ | (\bar{u} b) | \bar{B}^0 \rangle \left\{ (V_{ub} V_{us}^* a_1 - V_{tb} V_{ts}^* a_4) \langle \Lambda \bar{p} | (\bar{s} u) | 0 \rangle \right. \\
& \left. + 2a_6 V_{tb} V_{ts}^* \frac{(p_\Lambda + p_{\bar{p}})}{m_b - m_u} \langle \Lambda \bar{p} | \bar{s} (1 + \gamma_5) u | 0 \rangle \right\}. \tag{3.3}
\end{aligned}$$

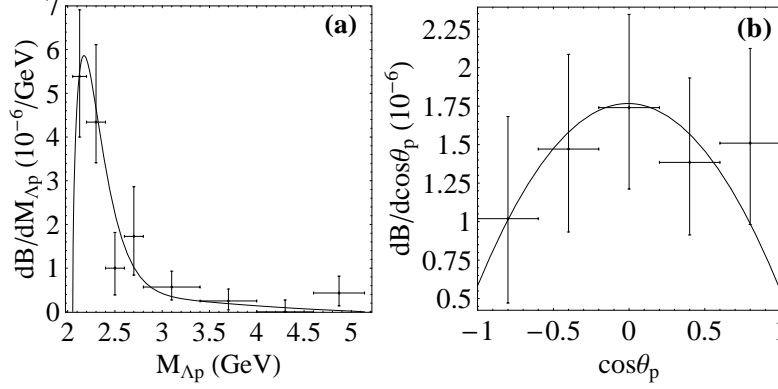


FIG. 4: (a) $\Lambda\bar{p}$ invariant mass spectrum and (b) the antiproton angular distribution in the $\Lambda\bar{p}$ rest frame for the decay $\bar{B}^0 \rightarrow \Lambda\bar{p}\pi^+$, where θ_p is the angle between the antiproton direction and the pion direction in the $\Lambda\bar{p}$ rest frame. Experimental data are taken from [21] and the theoretical curves are from [55].

For the matrix element of scalar and pseudoscalar densities,

$$\langle \Lambda\bar{p} | \bar{s}(1 + \gamma_5)u | 0 \rangle = f_S(t)\bar{u}_\Lambda v_{\bar{p}} + g_P(t)\bar{u}_\Lambda \gamma_5 v_{\bar{p}}, \quad (3.4)$$

the form factors $f_S(t)$ and $g_P(t)$ can be related to $f_1^{\Lambda p}(t)$ and $g_{1,3}^{\Lambda p}(t)$ via equations of motion. Based on the pQCD counting rule [54] which gives rise to the leading power in the large- t fall-off of the form factor by counting the number of gluon exchanges necessary to distribute the large momentum transfer to all constituents, the form factor generally has the asymptotic form

$$F(t) \rightarrow \frac{a}{t^2} + \frac{b}{t^3} \quad (3.5)$$

in the limit of large t , where $F(t) = f_i(t), g_i(t), f_S(t), g_P(t)$.

Fig. 4 shows the dibaryon mass spectrum and the angular distribution in the $\Lambda\bar{p}$ rest frame. The threshold enhancement effect depicted in Fig. 4(a) is closely related to the asymptotic behavior of various form factors, namely, they fall off fast with the dibaryon invariant mass. A detailed study in [55] shows that the differential decay rate for $\Lambda\bar{p}\pi^+$ should be in the form of a parabola that opens downward. This is indeed confirmed by experiment (Fig. 4(b)) where it is clear that the pion has no preference for its correlation with the Λ or the \bar{p} . This feature can be understood as follows. Since the dibaryon invariant mass in the B rest frame is given by

$$M_{\Lambda\bar{p}}^2 = m_\Lambda^2 + m_{\bar{p}}^2 + 2(E_\Lambda E_{\bar{p}} - |\vec{p}_\Lambda| |\vec{p}_{\bar{p}}| \cos \theta_{\Lambda\bar{p}}), \quad (3.6)$$

threshold enhancement implies that the baryon pair Λ and \bar{p} tend to move collinearly in this frame, i.e. $\theta_{\Lambda\bar{p}} \rightarrow 0$. In the penguin diagram responsible for $\bar{B}^0 \rightarrow \Lambda\bar{p}\pi^+$, both Λ and \bar{p} pick up energetic s and \bar{u} quarks, respectively, from the b decay. When the system is boosted to the $\Lambda\bar{p}$ rest frame, the pion is moving away from the dibaryon system. Therefore, the distribution should be symmetric. In contrast, the argument in [35] that the \bar{p} and π^+ are neighbors in the fragmentation chain so that the π^+ is correlated more strongly to the \bar{p} than to the Λ (or $\langle m_{\bar{p}\pi} \rangle < \langle m_{\Lambda\pi} \rangle$) will lead to an asymmetric angular distribution. Evidently, this feature is not borne out by experiment.

B. Decays involving $B \rightarrow \mathcal{B}_1 \bar{\mathcal{B}}_2$ transition

Apart from the purely transition-induced decays such as $\bar{B}^0 \rightarrow D^{(*)0} p \bar{p}$, $\bar{B}^0 \rightarrow \Sigma_c^{++} \bar{p} \pi^-$, most decays receive both current- and transition-induced contributions, e.g. $B^- \rightarrow p \bar{p} K^-, p \bar{p} \pi^-, \Lambda \bar{\Lambda} K^-, \Lambda_c^+ \bar{p} \pi^-$ and $\bar{B}^0 \rightarrow p \bar{p} K_S$. The phenomenon of threshold enhancement has been observed in all these modes.

The factorizable amplitude for the transition-induced process $\langle M | (\bar{q}_3 q_2) | 0 \rangle \langle \mathcal{B}_1 \bar{\mathcal{B}}_2 | (\bar{q}_1 b) | \bar{B} \rangle$ can be further simplified to

$$\langle P | (V \pm A)_\mu | 0 \rangle \langle \mathcal{B}_1 \bar{\mathcal{B}}_2 | (V - A)^\mu | \bar{B} \rangle = \pm i f_P \langle \mathcal{B}_1 \bar{\mathcal{B}}_2 | S + P | \bar{B} \rangle \quad (3.7)$$

for the case that the emitted meson is a pseudoscalar one. In this case, the matrix element of $\bar{B} \rightarrow \mathcal{B}_1 \bar{\mathcal{B}}_2$ can be parametrized in terms of four unknown 3-body form factors as

$$\langle \mathcal{B}_1 \bar{\mathcal{B}}_2 | S \pm P | \bar{B} \rangle = i \bar{u} \left[F_A^{\bar{B} \rightarrow \mathcal{B}_1 \bar{\mathcal{B}}_2} \not{p} \gamma_5 + F_P^{\bar{B} \rightarrow \mathcal{B}_1 \bar{\mathcal{B}}_2} \gamma_5 \pm (F_V^{\bar{B} \rightarrow \mathcal{B}_1 \bar{\mathcal{B}}_2} \not{p} + F_S^{\bar{B} \rightarrow \mathcal{B}_1 \bar{\mathcal{B}}_2}) \right] v. \quad (3.8)$$

It has been argued in [43] that in the asymptotic $t \rightarrow \infty$ limit, the pQCD counting rule implies

$$F_{V,A}^{\bar{B} \rightarrow \mathcal{B}_1 \bar{\mathcal{B}}_2} \rightarrow \frac{1}{t^3}, \quad F_P^{\bar{B} \rightarrow \mathcal{B}_1 \bar{\mathcal{B}}_2} \rightarrow \frac{1}{t^4} \quad (3.9)$$

as it needs three hard gluon exchanges to distribute the large momentum transfer released from the $b \rightarrow q$ transition. Consequently, just as the current-induced processes, the threshold enhancement effect is linked to the asymptotic behavior of the form factors. However, there are two reasons that the momentum dependence of the 3-body form factors cannot depend solely on the dibaryon invariant mass as proposed by Eq. (3.9). First, no threshold enhancement is observed in the decay mode $\Sigma_c(2455)^{++} \bar{p} \pi^-$ [26]. Second, the momentum dependence of form factors on the dibaryon mass will lead to a symmetric angular distribution similar to Fig. 4(b), which is in sharp contradiction to experiment for e.g. $B^- \rightarrow p \bar{p} K^-, B^- \rightarrow \Lambda_c^+ \bar{p} \pi^-$ and $\bar{B}^0 \rightarrow \Lambda \bar{p} \gamma$ where the angular distributions are obviously asymmetric (Fig. 5). In short, for the 3-body matrix element $\langle \mathcal{B}_1(p_1) \bar{\mathcal{B}}_2(p_2) | S \pm P | \bar{B}(p_B) \rangle$, the form factors in general depend not only on the invariant mass $t = (p_1 + p_2)^2$ of the dibaryon but also on the momentum transfer $(p_1 + p_3)^2$ or $(p_2 + p_3)^2$ where $p_3 = p_B - p_1 - p_2$.

Angular distributions of the baryon in the dibaryon rest frame have also been measured in $p \bar{p} K^-, p \bar{p} K_S$ and $\Lambda_c^+ \bar{p} \pi^-$ modes. The measurements of the correlation of the meson with the baryon provide the information on the form-factor momentum dependence. For $\bar{B} \rightarrow \mathcal{B}_1 \bar{\mathcal{B}}_2 M$, one can define the angular asymmetry as

$$A = \frac{N_+ - N_-}{N_+ + N_-}, \quad (3.10)$$

where N_+ and N_- are the events with $\cos \theta > 0$ and $\cos \theta < 0$, respectively, with θ being the angle between the meson direction and the antibaryon $\bar{\mathcal{B}}_2$ direction in the dibaryon rest frame. The angular asymmetry is measured to be $-0.59^{+0.08}_{-0.07}$, 0.32 ± 0.14 , and $0.36^{+0.23}_{-0.20}$ for $B^- \rightarrow p \bar{p} K^-, \Lambda_c^+ \bar{p} \pi^-, \Lambda \bar{p} \gamma$, respectively. Experimental measurements indicate that, in the baryon-antibaryon rest frame, the outgoing meson or the photon tends to emerge parallel to the antibaryon for $B^- \rightarrow \Lambda_c^+ \bar{p} \pi^-, \Lambda \bar{p} \gamma$ and to the baryon for $B^- \rightarrow p \bar{p} K^-$. As we shall see, a stronger correlation of the meson to the antibaryon than to the baryon in the dibaryon rest frame is expected in the pQCD picture for B decay. Hence, the opposite correlation effect seen in $B^- \rightarrow p \bar{p} K^-$ by BarBar and Belle to be discussed below is astonishing and entirely unexpected.

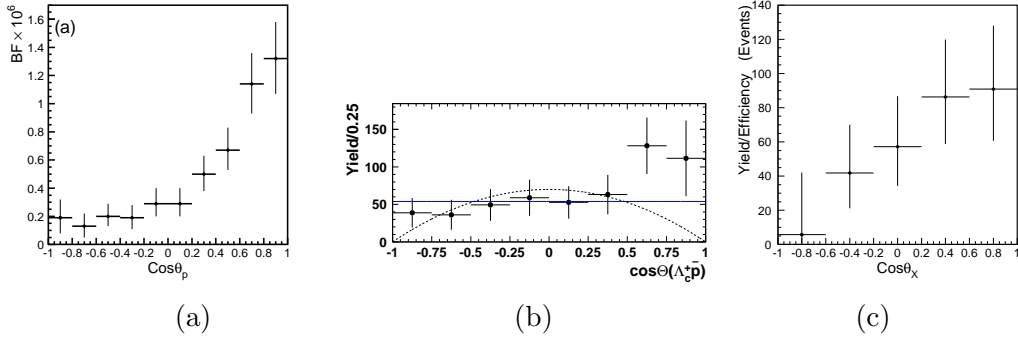


FIG. 5: Angular distributions of (a) the proton for $B^- \rightarrow p\bar{p}K^-$ [20] and the antiproton for (b) $\Lambda_c^+ \bar{p}\pi^-$ [14] and (c) $\Lambda\bar{p}\gamma$ [63] modes. Measurements are done in the dibaryon rest frame. θ_p in (a) is the angle between the proton direction and the kaon direction, while Θ in (b) (θ_X in (c)) is the angle between the antiproton and the pion (photon).

In the absence of theoretical guidance for the form factors in the three-body matrix element (3.8), one may consider a phenomenological pole model at the hadron level as put forward in [36]. The main assumption of the pole model is that the dominant contributions arise from the low-lying baryon and meson intermediate states. As we shall see, the meson pole diagrams are usually related to the vacuum to $\mathcal{B}_1\bar{\mathcal{B}}_2$ transition form factors and hence responsible for threshold enhancement, whereas the baryon pole diagrams account for the correlation of the outgoing meson with the baryon.

Consider a typical meson pole diagram, say, Fig. 3(b). The corresponding rate is proportional to

$$\Gamma \propto \int \dots \left| \frac{g_{M'\mathcal{B}_1\bar{\mathcal{B}}_2}}{m_{12}^2 - m_{M'}^2} \right|^2 dm_{12}^2 dm_{23}^2, \quad (3.11)$$

where $m_{ij}^2 = (p_i + p_j)^2$ with $p_3 = p_M$ and M' is the mass of the meson pole. It is clear that the meson propagator is maximal when the dibaryon invariant mass is near threshold, i.e. $m_{12} \sim m_1 + m_2$. In general, the strong coupling at the $M'\mathcal{B}_1\bar{\mathcal{B}}_2$ vertex can be related to the vacuum to $\mathcal{B}_1\bar{\mathcal{B}}_2$ form factors via

$$g_{M'\mathcal{B}_1\bar{\mathcal{B}}_2}(t) = \frac{t - m_{M'}^2}{f_{M'} m_{M'}} f_{\mathcal{B}_1\bar{\mathcal{B}}_2}(t) \quad (3.12)$$

with $t = m_{12}^2$. Then the current-induced decay amplitude is reproduced and threshold enhancement is connected to the asymptotic behavior of the form factors.

Next consider a baryon pole diagram such as the one in Fig. 3(a),

$$\Gamma \propto \int \dots \left| \frac{g_{M\mathcal{B}_1\mathcal{B}_b}}{m_{13}^2 - m_{\mathcal{B}_b}^2} \right|^2 dm_{12}^2 dm_{23}^2. \quad (3.13)$$

Since in the dibaryon rest frame

$$m_{13}^2 = m_1^2 + m_M^2 + 2(E_1 E_M - p_{c.m.}^2 \cos \theta_{13}), \quad (3.14)$$

where $p_{c.m.}$ is the c.m. momentum and since $m_{\mathcal{B}_b} \gg m_{\mathcal{B}}, m_M$, it is clear that the decay rate becomes prominent when $\cos \theta_{13} \rightarrow -1$; that is, when the baryon is moving antiparallel to the meson. Therefore, the baryon pole diagram always implies that *the antibaryon tends to emerge parallel to the outgoing meson*. Intuitively, the observation that the meson is correlated more strongly to the $\bar{\mathcal{B}}_2$ than to the \mathcal{B}_1 also can be understood in the following manner. Since in the B rest frame

$$m_{12}^2 = m_1^2 + m_2^2 + 2(E_1 E_2 - |\vec{p}_1| |\vec{p}_2| \cos \theta_{12}), \quad (3.15)$$

threshold enhancement implies that the baryon pair \mathcal{B}_1 and $\bar{\mathcal{B}}_2$ tend to move collinearly in this frame, i.e. $\theta_{12} \rightarrow 0$. From Fig. 3(a) we see that the \mathcal{B}_1 is moving faster than $\bar{\mathcal{B}}_2$ as the former picks up an energetic quark from the b decay. When the system is boosted to the $\mathcal{B}_1 \bar{\mathcal{B}}_2$ rest frame, $\bar{\mathcal{B}}_2$ and M are moving collinearly away from the \mathcal{B}_1 .

C. $B^- \rightarrow p\bar{p}K^-$

This mode has been measured by BaBar [11] and Belle [21] with the averaged branching ratio $(6.10 \pm 0.48) \times 10^{-6}$ (Table III). Threshold enhancement in the dibaryon mass distribution is also observed by both B factories. Recently, Belle has studied the angular distribution in the baryon-antibaryon pair rest frame [21], while BaBar has measured the Dalitz plot asymmetry in the decay $B^- \rightarrow p\bar{p}K^-$ [11].

Based on the pole model and the intuitive argument described before, the K^- in the $p\bar{p}$ rest frame is expected to emerge parallel to \bar{p} . However, the Belle observation is other around [21]: the K^- is preferred to move collinearly with the proton in the $p\bar{p}$ rest frame. Instead of measuring angular distributions, BaBar has studied the Dalitz plot asymmetry in the invariant masses m_{pK} and $m_{\bar{p}K}$ and found that $m_{pK} < m_{\bar{p}K}$. This is consistent with the Belle result because in the $p\bar{p}$ rest frame

$$\begin{aligned} m_{pK}^2 &= m_p^2 + m_K^2 + 2(E_p E_K - |\vec{p}_K| p_{cm} \cos \theta_p), \\ m_{\bar{p}K}^2 &= m_{\bar{p}}^2 + m_K^2 + 2(E_{\bar{p}} E_K + |\vec{p}_K| p_{cm} \cos \theta_p), \end{aligned} \quad (3.16)$$

where θ_p is the angle between the K^- and the p directions. Hence, the observation of $m_{pK} < m_{\bar{p}K}$ implies that θ_p is preferred to be small. Therefore, K^- and p tend to move collinearly in the $p\bar{p}$ rest frame.

The correlation of the kaon with the proton observed by BaBar and Belle is in contradiction to the naive expectation. Near the threshold area, the proton and the antiproton move collinearly in the B rest frame. Again, $m_{pK} < m_{\bar{p}K}$ indicates that the p is moving slower than the \bar{p} . However, the dominant factorizable penguin diagram for $B^- \rightarrow p\bar{p}K^-$ (Fig. 6(a)) implies a p moving faster than \bar{p} . It has been argued in [35] that since the \bar{u} quark in the K^- is associated with a u quark in the p (Fig. 6), it leads to a strong $p - K^-$ angular correlation and $m_{pK} < m_{\bar{p}K}$. However, this argument is valid only for Fig. 6(c) where \bar{p} is moving faster than p . For the dominant penguin diagram 6(a), pole model or the intuitive argument leads to an opposite correlation between the kaon and the proton. Since the penguin annihilation diagram Fig. 6(c) cannot be the dominant contribution to $B^- \rightarrow p\bar{p}K^-$ as it is suppressed relative to the factorizable penguin diagram by $1/m_B$, the observed angular distribution becomes quite tantalizing.

The aforementioned puzzle could indicate that the $p\bar{p}$ system is produced from some intermediate states, such as the glueball and the baryonium, a $p\bar{p}$ bound state. This may change the

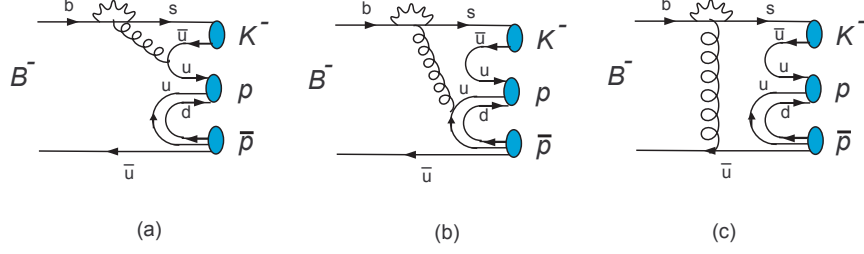


FIG. 6: Penguin diagram contributions to $B^- \rightarrow p\bar{p}K^-$.

correlation pattern. This possibility is currently under study in [56]. It is likely that the new mechanism responsible for the anomalous correlation effect observed in $p\bar{p}K^-$ only occurs in the penguin-dominated modes, but not in the tree-dominated decay such as $B^- \rightarrow p\bar{p}\pi^-$. Hence, experimentally it is very important to study the angular distributions of the baryon for $p\bar{p}X$ with $X = K^{*+}, K^0, K^{*0}, \pi^-$ and $\Lambda\bar{\Lambda}K^-$ modes.

D. Other salient features

Many of other 3-body baryonic B decays have been studied in [36, 37, 42, 43, 44, 45, 57]. Because of space limitation, we will focus on a few of the prominent features of them:

- Contrary to $\bar{B}^0 \rightarrow D^{(*)+}n\bar{p}$ decays where the D^{*+}/D^+ production ratio is anticipated to be of order 3, the D^{*0}/D^0 production ratio in color suppressed $\bar{B}^0 \rightarrow D^{(*)0}p\bar{p}$ decays is consistent with unity experimentally (see Table IV). It is shown in [45] that the similar rates for $D^0p\bar{p}$ and $D^{*0}p\bar{p}$ can be understood within the framework of the pole model as the former is dominated by the axial-vector meson states, whereas the other modes proceed mainly through the vector meson poles.
- The spectrum of $\bar{B} \rightarrow D^0p\bar{p}$ is predicted to have a hump at large $p\bar{p}$ invariant mass $m_{p\bar{p}} \sim 2.9$ GeV [45] (see Fig. 7), which needs to be checked by forthcoming experiments. As for the correlation, it is expected that $\langle m_{D\bar{p}} \rangle < \langle m_{Dp} \rangle$ according to the discussion shown in Sec.3.B, whereas it is other way around, namely, $\langle m_{Dp} \rangle < \langle m_{D\bar{p}} \rangle$ in the fragmentation picture of [35].
- Charmless decays $B^- \rightarrow p\bar{p}K^-(K^{*-})$ are penguin-dominated. It is naively expected that $p\bar{p}K^{*-} < p\bar{p}K^-$ due to the absence of a_6 and a_8 penguin terms contributing to the former. The Belle observation of a large rate for the K^* production (see Table III) is thus unexpected. Also, it is non-trivial to understand the observed sizable rate of $\bar{B}^0 \rightarrow p\bar{p}\bar{K}^0$ [36, 44].
- The relations among several penguin-dominated three-body baryonic decays

$$\begin{aligned}
 \Gamma(\bar{B}^0 \rightarrow \Sigma^- \bar{n} \pi^+) &= 2\Gamma(\bar{B}^0 \rightarrow \Sigma^0 \bar{p} \pi^+) = 2\Gamma(B^- \rightarrow \Sigma^- \bar{n} \pi^0) = 4\Gamma(B^- \rightarrow \Sigma^0 \bar{p} \pi^0), \\
 \Gamma(\bar{B}^0 \rightarrow \Xi^0 \bar{\Sigma}^- \pi^+) &= 2\Gamma(B^- \rightarrow \Xi^0 \bar{\Sigma}^- \pi^0) = 2\Gamma(\bar{B}^0 \rightarrow \Xi^- \bar{\Sigma}^0 \pi^+) = 4\Gamma(B^- \rightarrow \Xi^- \bar{\Sigma}^0 \pi^0), \\
 \Gamma(\bar{B}^0 \rightarrow \Lambda \bar{p} \pi^+) &= 2\Gamma(B^- \rightarrow \Lambda \bar{p} \pi^0),
 \end{aligned} \tag{3.17}$$

have been derived based on isospin symmetry and factorization [44]. Hence, the factorization assumption can be tested by measuring the above relations.

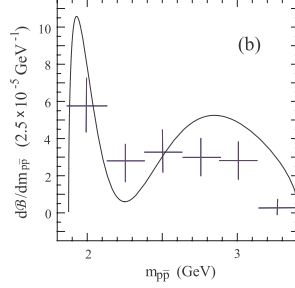


FIG. 7: The predicted $p\bar{p}$ invariant mass distribution of $\bar{B}^0 \rightarrow D^0 p\bar{p}$ [45]. The experimental data are taken from [25].

- The three-body doubly charmed baryonic decay $B \rightarrow \Lambda_c \bar{\Lambda}_c K$ has been observed recently by Belle with the branching ratio of order 7×10^{-4} (see Table IV). Since this mode is color-suppressed and its phase space is highly suppressed, the naive estimate of $\mathcal{B} \sim 10^{-8}$ is too small by four to five orders of magnitude compared to experiment. It was originally conjectured in [48] that the great suppression for the $\Lambda_c^+ \bar{\Lambda}_c^- K$ production can be alleviated provided that there exists a narrow hidden charm bound state with a mass near the $\Lambda_c \bar{\Lambda}_c$ threshold. This possibility is plausible, recalling that many new charmonium-like resonances with masses around 4 GeV starting with $X(3872)$ [49] and so far ending with $Y(4260)$ [50] have been recently observed by BaBar and Belle. This new state that couples strongly to the charmed baryon pair can be searched for in B decays and in $p\bar{p}$ collisions by studying the mass spectrum of $D^{(*)} \bar{D}^{(*)}$ or $\Lambda_c \bar{\Lambda}_c$. However, no new resonance with a mass near the $\Lambda_c \bar{\Lambda}_c$ threshold was found (see Fig. 3 in version 2 of [27]). This implies the failure of naive factorization for this decay mode and may hint at the importance of nonfactorizable contributions such as final-state effects. For example, the weak decay $B \rightarrow D^{(*)} \bar{D}_s^{(*)}$ followed by the rescattering $D^{(*)} \bar{D}_s^{(*)} \rightarrow \Lambda_c \bar{\Lambda}_c K$ or the decay $B \rightarrow \Xi_c \bar{\Lambda}_c$ followed by $\Xi_c \bar{\Lambda}_c \rightarrow \Lambda_c \bar{\Lambda}_c K$ may explain the large rate observed for $B \rightarrow \Lambda_c \bar{\Lambda}_c K$.
- Triple product correlations (TCP) in three-body baryonic B decays can be studied to test T violation. Unlike the usual direct CP asymmetry, the T -odd asymmetry due to TCP does not vanish even in the absence of strong phases. It has been estimated in [58] that T violation induced from the asymmetry in $\vec{s}_\Lambda \cdot (\vec{p}_{\bar{p}} \times \vec{p}_\Lambda)$ in $\bar{B}^0 \rightarrow \Lambda \bar{p} \pi^+$ decay can be as large as 10%, while CP asymmetry is only at 1% level.

IV. RADIATIVE BARYONIC B DECAYS

Naively it appears that the bremsstrahlung process will lead to $\Gamma(B \rightarrow \mathcal{B}_1 \bar{\mathcal{B}}_2 \gamma) \sim \mathcal{O}(\alpha_{\text{em}}) \Gamma(B \rightarrow \mathcal{B}_1 \bar{\mathcal{B}}_2)$ with α_{em} being an electromagnetic fine-structure constant and hence the radiative baryonic B decay is further suppressed than the two-body counterpart, making its observation very difficult at the present level of sensitivity for B factories. However, there is an important short-distance electromagnetic penguin transition $b \rightarrow s \gamma$. Owing to the large top quark mass, the amplitude of $b \rightarrow s \gamma$ is neither quark mixing nor loop suppressed. Moreover, it is largely enhanced by QCD corrections. As a consequence, the short-distance contribution due to the electromagnetic penguin

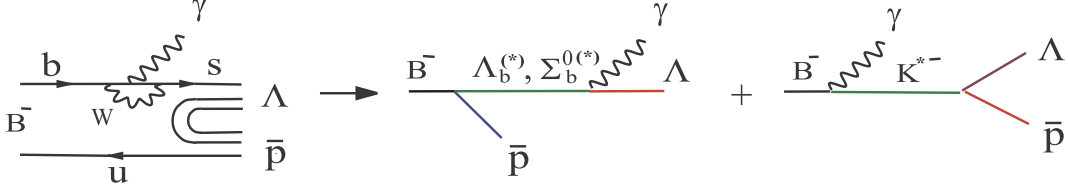


FIG. 8: Quark and pole diagrams for $B^- \rightarrow \Lambda \bar{p} \gamma$.

diagram dominates over the bremsstrahlung. This phenomenon is quite unique to the bottom hadrons which contain a heavy b quark; such a magic short-distance enhancement does not occur in the systems of charmed and strange hadrons.

Since a direct evaluation of this radiative decay is difficult as it involves an unknown 3-body matrix element $M_{\mu\nu} = \langle \Lambda \bar{p} | \bar{s} \sigma_{\mu\nu} (1 + \gamma_5) b | B^- \rangle$, we shall instead evaluate the corresponding diagrams known as pole diagrams at the hadron level (see Fig. 8). In principle, there exist many possible baryon and meson pole contributions. The main assumption of the pole model is that the dominant contributions arise from the low-lying baryon and meson intermediate states. For $B^- \rightarrow \Lambda \bar{p} \gamma$, the relevant intermediate states are $\Lambda_b^{(*)}$, $\Sigma_b^{0(*)}$ and K^* .

The predicted branching ratios for $B^- \rightarrow \Sigma^0 \bar{p} \gamma$, $\Xi^0 \bar{\Sigma}^- \gamma$ and $\Xi^- \bar{\Lambda} \gamma$ decays are summarized in Table VIII.³ Decay rates for the other modes can be obtained via the relations [59] (see also [61, 62])

$$\begin{aligned} \Gamma(B^- \rightarrow \Sigma^- \bar{n} \gamma) &= 2\Gamma(B^- \rightarrow \Sigma^0 \bar{p} \gamma) = 2\Gamma(\bar{B}^0 \rightarrow \Sigma^0 \bar{n} \gamma) = \Gamma(\bar{B}^0 \rightarrow \Sigma^+ \bar{p} \gamma), \\ \Gamma(\bar{B}^0 \rightarrow \Xi^- \bar{\Sigma}^+ \gamma) &= 2\Gamma(B^- \rightarrow \Xi^- \bar{\Sigma}^0 \gamma) = 2\Gamma(\bar{B}^0 \rightarrow \Xi^0 \bar{\Sigma}^0 \gamma) = \Gamma(B^- \rightarrow \Xi^0 \bar{\Sigma}^- \gamma), \\ \Gamma(\bar{B}^0 \rightarrow \Lambda \bar{n} \gamma) &= \Gamma(B^- \rightarrow \Lambda \bar{p} \gamma), \quad \Gamma(\bar{B}^0 \rightarrow \Xi^0 \bar{\Lambda} \gamma) = \Gamma(B^- \rightarrow \Xi^- \bar{\Lambda} \gamma). \end{aligned} \quad (4.1)$$

It is interesting to notice that the $\Sigma^0 \bar{p} \gamma$ mode, which was previously argued to be very suppressed due to the smallness of the strong coupling $g_{\Sigma_b \rightarrow B^- p}$ [59], receives the dominant contribution from the K^* pole diagram and its branching ratio is consistent with that obtained in [61]. In contrast, the mode $\Xi^0 \bar{\Sigma}^- \gamma$ is dominated by the baryon pole contribution. Meson and baryon intermediate state contributions are comparable in $\Lambda \bar{p} \gamma$ and $\Xi^- \bar{\Lambda} \gamma$ modes except that they interfere constructively in the former but destructively in the latter. Recently, Belle [63] has made the first observation of radiative hyperonic B decay $B^- \rightarrow \Lambda \bar{p} \gamma$ with the result

$$\mathcal{B}(B^- \rightarrow \Lambda \bar{p} \gamma) = (2.16_{-0.53}^{+0.58} \pm 0.20) \times 10^{-6}. \quad (4.2)$$

In addition to the first observation of $\Lambda \bar{p} \gamma$, the decay $B^- \rightarrow \Xi^0 \bar{\Sigma}^- \gamma$ at the level of 6×10^{-7} may be accessible to B factories in the future.

In addition to the threshold enhancement effect observed in the differential branching fraction of $\Lambda \bar{p} \gamma$ (Fig. 9.(a)), Belle has also measured the angular distribution of the antiproton in the $\Lambda \bar{p}$ system (Fig. 9.(b)), where θ_p is the angle between the antiproton direction and the photon direction in the $\Lambda \bar{p}$ rest frame. It is clear that the Λ tends to emerge opposite the direction of the

³ In the previous work [59], the meson pole contributions which are *a priori* not necessarily small have been neglected. It is updated in [60] including some improved input parameters such as strong couplings.

TABLE VIII: Branching ratios and angular asymmetries defined in Eq. (3.10) for radiative baryonic B decays.

| Mode | Baryon pole | Meson pole | Br(total) | Angular asymmetry |
|---|----------------------|----------------------|----------------------|-------------------|
| $B^- \rightarrow \Lambda \bar{p} \gamma$ | 7.9×10^{-7} | 9.5×10^{-7} | 2.6×10^{-6} | 0.25 |
| $B^- \rightarrow \Sigma^0 \bar{p} \gamma$ | 4.6×10^{-9} | 2.5×10^{-7} | 2.9×10^{-7} | 0.07 |
| $B^- \rightarrow \Xi^0 \bar{\Sigma}^- \gamma$ | 7.5×10^{-7} | 1.6×10^{-7} | 5.6×10^{-7} | 0.43 |
| $B^- \rightarrow \Xi^- \bar{\Lambda} \gamma$ | 1.6×10^{-7} | 2.4×10^{-7} | 2.2×10^{-7} | 0.13 |

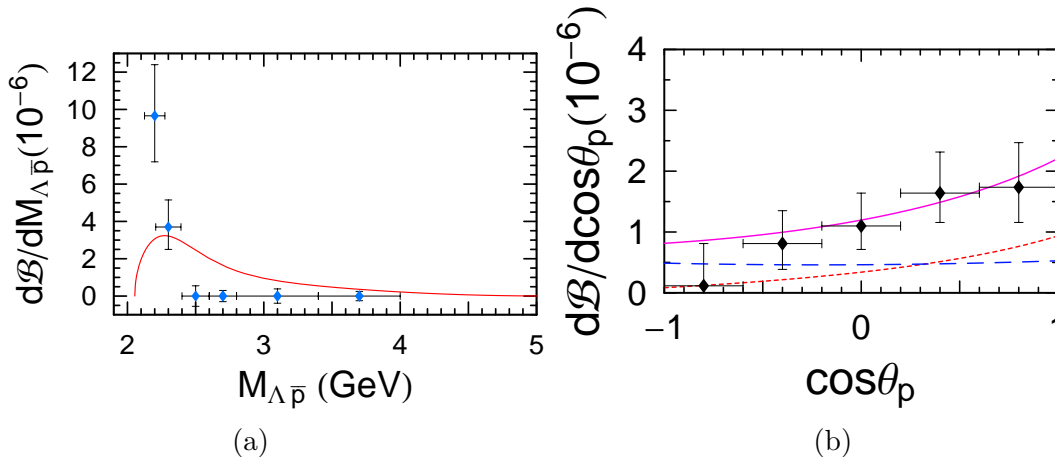


FIG. 9: (a) $\Lambda \bar{p}$ invariant mass distribution and (b) the angular distribution of the antiproton in the baryon pair system for $B^- \rightarrow \Lambda \bar{p} \gamma$, where θ_p is the angle between the antiproton direction and the photon direction in the $\Lambda \bar{p}$ rest frame. The dotted, dashed and solid curves stand for baryon pole, meson pole and total contributions, respectively. Data are taken from [63].

photon. The angular asymmetry is measured by Belle to be $A = 0.36^{+0.23}_{-0.20}$ for $B^- \rightarrow \Lambda \bar{p} \gamma$ [63]. The meson pole diagram is responsible for low-mass enhancement and does not show a preference for the correlation between the baryon pair and the photon (see the dashed curve in Fig. 9). Our prediction $A = 0.25$ (see Table VIII) is consistent with experiment.

V. CONCLUSION

Experimental and theoretical progresses in exclusive baryonic B decays in the past five years are impressive. The threshold peaking effect in baryon pair invariant mass is one of the key ingredients in understanding three-body decays. Weak radiative baryonic decays mediated by the electromagnetic penguin process $b \rightarrow s \gamma$ are studied and some of them are readily accessible experimentally. There are two unsolved puzzles with the 3-body decays: one is the anomalous correlation effect observed in $B^- \rightarrow p \bar{p} K^-$ decay and the other is the unexpectedly large rate observed for $B \rightarrow \Lambda_c \bar{\Lambda}_c K$. The former may indicate that $p \bar{p}$ is coupled to some intermediate states, while the latter implies the failure of naive factorization for $\Lambda \bar{\Lambda} K$ modes and may hint at the importance of final-state rescattering effects. Experimentally, it is very important to measure the

correlation of the outgoing meson with the baryon in three-body baryonic B decays in order to gain further dynamical insight and to discriminate between different models.

Acknowledgments

I'm grateful to Chun-Khiang Chua, Shang-Yuu Tsai and Kwei-Chou Yang for fruitful collaboration, to Min-ru Wang for valuable discussions and to Otto Kong for organizing this excellent conference.

-
- [1] X.Y. Pham, Phys. Rev. Lett. **45**, 1663 (1980).
 - [2] ARGUS Collaboration, H. Albrecht *et al.*, Phys. Lett. B **209**, 119 (1988).
 - [3] CLEO Collaboration, C. Bebek *et al.*, Phys. Rev. Lett. **62**, 2436 (1989).
 - [4] J.G. Körner, Z. Phys. C **43**, 165 (1989).
 - [5] N.G. Deshpande, J. Trampetic, and A. Soni, Mod. Phys. Lett. A **3**, 749 (1988).
 - [6] M. Jarfi *et al.*, Phys. Rev. D **43**, 1599 (1991); Phys. Lett. B **237**, 513 (1990).
 - [7] V. Chernyak and I. Zhitnitsky, Nucl. Phys. B **345**, 137 (1990).
 - [8] P. Ball and H.G. Dosch, Z. Phys. C **51**, 445 (1991).
 - [9] M. Gronau and J.L. Rosner, Phys. Rev. D **37**, 688 (1988); G. Eilam, M. Gronau, and J.L. Rosner, *ibid.* **39**, 819 (1989); X.G. He, B.H.J. McKellar, and D.d. Wu, *ibid.* **41**, 2141 (1990); S.M. Sheikholeslami and M.P. Khanna, *ibid.* **44**, 770 (1991); S.M. Sheikholeslami, G.K. Sindana, and M.P. Khanna, Int. J. Mod. Phys. A **7**, 1111 (1992).
 - [10] BaBar Collaboration, B. Aubert *et al.*, Phys. Rev. D **69**, 091503 (2004).
 - [11] BaBar Collaboration, B. Aubert *et al.*, Phys. Rev. D **72**, 051101 (2005).
 - [12] Belle Collaboration, M.C. Chang *et al.*, Phys. Rev. D **71**, 072007 (2005).
 - [13] CLEO Collaboration, A. Bornheim *et al.*, Phys. Rev. D **68**, 052002 (2003); T.E. Coan *et al.*, *ibid.* **59**, 111101 (1999).
 - [14] Belle Collaboration, N. Gabyshev *et al.*, hep-ex/0409005.
 - [15] Belle Collaboration, N. Gabyshev *et al.*, Phys. Rev. Lett. **90**, 121802 (2003).
 - [16] Belle Collaboration, R. Chistov *et al.*, hep-ex/0510074.
 - [17] CLEO Collaboration, S.A. Dytman *et al.*, Phys. Rev. D **66**, 091101 (2002).
 - [18] H.Y. Cheng and B. Tseng, Phys. Rev. D **48**, 4188 (1993).
 - [19] Particle Data Group, S. Eidelman *et al.*, Phys. Lett. B **592**, 1 (2004).
 - [20] Belle Collaboration, M.Z. Wang *et al.*, Phys. Rev. Lett. **90**, 201802 (2003); *ibid.* **92**, 131801 (2004); Y.J. Lee *et al.*, Phys. Rev. Lett. **93**, 211801 (2004).
 - [21] Belle Collaboration, M.Z. Wang *et al.*, Phys. Lett. B **617**, 141 (2005).
 - [22] Belle Collaboration, K. Abe *et al.*, Phys. Rev. Lett. **88**, 181803 (2002).
 - [23] BaBar Collaboration, B. Aubert *et al.*, hep-ex/0408035.
 - [24] BaBar Collaboration, B. Aubert *et al.*, Phys. Rev. Lett. **90**, 231801 (2003).
 - [25] Belle Collaboration, N. Gabyshev *et al.*, Phys. Rev. D **66**, 091102 (2002); K. Abe *et al.*, Phys. Rev. Lett. **89**, 151802 (2002).
 - [26] Belle Collaboration, K. Abe *et al.*, BELLE-CONF-0467.
 - [27] Belle Collaboration, N. Gabyshev *et al.*, hep-ex/0508015.

- [28] Belle Collaboration, Q.L. Xie *et al.*, Phys. Rev. D **72**, 051105 (2005).
- [29] CLEO Collaboration, S. Anderson *et al.*, Phys. Rev. Lett. **86**, 2732 (2001).
- [30] BES Collaboration, J.Z. Bai *et al.*, Phys. Rev. Lett. **91**, 022001 (2003).
- [31] BES Collaboration, M. Ablikim *et al.*, Phys. Rev. Lett. **93**, 112002 (2004).
- [32] W.S. Hou and A. Soni, Phys. Rev. Lett. **86**, 4247 (2001).
- [33] BES Collaboration, M. Ablikim *et al.*, hep-ex/0508025.
- [34] C.K. Chua, W.S. Hou, and S.Y. Tsai, Phys. Lett. B **544**, 139 (2002).
- [35] J.L. Rosner, Phys. Rev. D **68**, 014004 (2003).
- [36] H.Y. Cheng and K.C. Yang, Phys. Rev. D **66**, 014020 (2002).
- [37] H.Y. Cheng and K.C. Yang, Phys. Rev. D **67**, 034008 (2003); *ibid.* **65**, 054028 (2002).
- [38] C.H. Chang and W.S. Hou, Eur. Phys. J. C **23**, 691 (2002).
- [39] Z. Luo and J.L. Rosner, Phys. Rev. D **67**, 094017 (2003).
- [40] C.K. Chua, Phys. Rev. D **68**, 074001 (2003).
- [41] M. Suzuki, J. Phys. G **31**, 755 (2005).
- [42] C.K. Chua, W.S. Hou, and S.Y. Tsai, Phys. Rev. D **65**, 034003 (2002); Phys. Lett. B **528**, 233 (2002).
- [43] C.K. Chua, W.S. Hou, and S.Y. Tsai, Phys. Rev. D **66**, 054004 (2002).
- [44] C.K. Chua and W.S. Hou, Eur. Phys. J. C **29**, 27 (2003).
- [45] H.Y. Cheng and K.C. Yang, Phys. Rev. D **66**, 094009 (2002).
- [46] H.Y. Cheng and K.C. Yang, Phys. Lett. B **533**, 271 (2002).
- [47] H.Y. Cheng and B. Tseng, Phys. Rev. D **46**, 1042 (1992); **55**, 1697(E) (1997).
- [48] H.Y. Cheng, C.K. Chua, and S.Y. Tsai, hep-ph/0512335.
- [49] S.K. Choi *et al.* [Belle Collaboration], Phys. Rev. Lett. **91**, 262001 (2003); D. Acosta *et al.* [CDF Collaboration], Phys. Rev. Lett. **93**, 072001 (2004); V.M. Abazov *et al.* [D0 Collaboration], Phys. Rev. Lett. **93**, 162002 (2004); B. Aubert *et al.* [BaBar Collaboration], Phys. Rev. D **71**, 071103 (2005).
- [50] B. Aubert *et al.* [BaBar Collaboration], Phys. Rev. Lett. **95**, 142001 (2005).
- [51] C.H. Chou, H.H. Shih, S.C. Lee, and H-n Li, Phys. Rev. D **65**, 074030 (2002).
- [52] G. Buchalla, I. Dunietz, and H. Yamamoto, Phys. Lett. B **364**, 188 (1995).
- [53] I. Dunietz, Phys. Rev. D **58**, 094010 (1998).
- [54] S.J. Brodsky and G.R. Farrar, Phys. Rev. D **11**, 1309 (1975).
- [55] S.Y. Tsai, “Study of Three-body Baryonic B Decays”, Ph.D. thesis, National Taiwan University (2005).
- [56] H.Y. Cheng, C.K. Chua, W.S. Hou, and S.Y. Tsai, in preparation.
- [57] C.Q. Geng and Y.K. Hsiao, Phys. Lett. B **619**, 305 (2005).
- [58] C.Q. Geng and Y.K. Hsiao, Phys. Rev. D **72**, 037901 (2005).
- [59] H.Y. Cheng and K.C. Yang, Phys. Lett. B **533**, 271 (2002).
- [60] H.Y. Cheng and K.C. Yang, Phys. Lett. B **633**, 533 (2006).
- [61] C.Q. Geng and Y.K. Hsiao, Phys. Lett. B **610**, 67 (2005).
- [62] Y. Kohara, Phys. Rev. D **70**, 097502 (2004).
- [63] Belle Collaboration, Y.J. Lee *et al.*, Phys. Rev. Lett. **95**, 061802 (2005).